




Cite this: *RSC Adv.*, 2018, 8, 41950

# Paper-based chemical reaction arrays as an effective tool for geographical indication of turmeric<sup>†</sup>

Monrawat Rauytanapanit,<sup>ab</sup> Thanyada Sukmanee,<sup>ac</sup> Kanet Wongravee<sup>ac</sup> and Thanit Praneenarat<sup>ab</sup> 

Geographical indications have gained increasing importance as a powerful marketing tool for highly valuable products especially foods. In this study, a unique and synergistic combination of chemical reaction arrays on paper and chemometric analysis was used to uncover geographical indication of turmeric, an important food ingredient in several cultures. The key to effective differentiation was based on the subtle differences in the compositions of compounds found in each sample, mainly curcumin and derivatives. When these compounds reacted with various reagents in the form of paper arrays, different optical and fluorescence profiles were generated, which can then be exploited by chemometrics. As a result, our strategy could provide up to 94% prediction accuracy without the need for any sophisticated instruments.

Received 8th November 2018  
 Accepted 8th December 2018

DOI: 10.1039/c8ra09248f

[rsc.li/rsc-advances](http://rsc.li/rsc-advances)

## Introduction

In the modern world, geographical indications (GI), or signs used to indicate a clear link between an attribute and the origin of a product, have become an important tool for the economies of communities producing highly desired products.<sup>1,2</sup> Prosciutto di Parma and Champagne are well-known examples of products that are protected by their GIs, leading to high economic values.<sup>1</sup> Interestingly, scientific methods especially chemical methods can offer several advantages to confirm GIs, thanks to their objective nature, and a wealth of efficient identification methods.<sup>3–5</sup> This has led to several investigations where chemical tools and knowledge, typically coupled with chemometrics, were employed to reveal and identify new GIs.<sup>6–11</sup> Examples include the discrimination of geographical origins of ginger by HPLC-DAD and chemometric treatment,<sup>6</sup> and the adoption of mineral composition as a tracer to identify lemons from the Messina region in Italy.<sup>7</sup> Given the success of this approach, it is likely that this trend can continue into other products, especially food and agricultural products.

Turmeric (*Curcuma longa*) is an Asia- and South East Asia-native plant, which belongs to the ginger family, Zingiberaceae. Similar to other plants in this family such as ginger or galangal, the rhizome of turmeric is usually used as spice and herbal supplement. The use for traditional medicine stemmed from the fact that the major compound in turmeric, curcumin (Fig. 1), was found to exhibit a wide range of biological activities.<sup>12–17</sup> Although there have been some reports that caution the possible false positive activities of curcumin,<sup>18,19</sup> it is unlikely that turmeric will be abandoned. This is because it has been firmly incorporated into traditional cuisines of many countries, especially curry dishes. Therefore, the knowledge of the origins of turmeric, which may be related to its medicinal or sensory properties, is still deemed to have great economic values for the food industry.

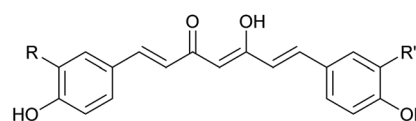
In regard to the chemistry of curcumin, this key compound usually exists as a mixture with its demethoxy derivatives (Fig. 1).<sup>12,14</sup> As a rare naturally occurring example of  $\alpha,\beta$ -unsaturated  $\beta$ -diketoheptanoid, curcumins possess unique structural features that, apart from their biological studies, were also investigated in other ways. For instance, its extensive  $\pi$ -

<sup>a</sup>Department of Chemistry, Faculty of Science, Chulalongkorn University, Phayathai Rd., Pathumwan, Bangkok, 10330, Thailand. E-mail: [thanit.p@chula.ac.th](mailto:thanit.p@chula.ac.th)

<sup>b</sup>The Chemical Approaches for Food Applications Research Group, Faculty of Science, Chulalongkorn University, Phayathai Rd., Pathumwan, Bangkok, 10330, Thailand

<sup>c</sup>Sensor Research Unit (SRU), Department of Chemistry, Faculty of Science, Chulalongkorn University, Phayathai Rd., Pathumwan, Bangkok, 10330, Thailand

<sup>†</sup> Electronic supplementary information (ESI) available: Origins of each turmeric samples, HPLC chromatograms, LC-MS data, preparations of reagents in the arrays, calibration plots of certain reagents, and additional chemometric protocols and data. See DOI: 10.1039/c8ra09248f



curcumin: R = OMe, R' = OMe  
 demethoxycurcumin: R = OMe, R' = H  
 bisdemethoxycurcumin: R = H, R' = H

Fig. 1 The structure of curcumin and common derivatives.



conjugation system results in curcumin being highly coloured, with a major absorption around 425 nm.<sup>20,21</sup> In addition, curcumins can strongly fluoresce as a green emission (550 nm) even upon an excitation by ordinary black light. This fascinating property of curcumins led to an adaptation as a safe dye for general purposes.<sup>22–24</sup>

Notably, the structural feature of curcumins also allows for diverse types of chemical modifications.<sup>14,25–32</sup> The most commonly known modification is the capability of curcumins to accommodate various metal ions, creating most commonly 2 : 1 ligand : metal complexes (Scheme 1).<sup>14</sup> Apart from showing different biological activities from free curcumins,<sup>14,25,33</sup> some metal-curcumin complexes showed significantly different photophysical properties, thus allowing the use of curcumins as sensors for these metal ions.<sup>26–30</sup> In addition, the reactions with the conjugated carbonyl system are possible, allowing the synthesis of derivatives from reagents such as 2,4-dinitrophenylhydrazine<sup>34–36</sup> (2,4-DNP, Scheme 1) and vanillin<sup>37,38</sup> – these compounds usually showed some changes in photophysical properties.

In this study, the photophysical changes of curcumins upon reacting with various reagents were explored as a means to differentiate and identify sources of turmeric. The key

hypothesis was that subtle differences in chemical components in each turmeric extract may affect the kinetics and thermodynamics of each reaction in different ways, depending on specific compositions of each extract. This can then be used as a differentiation method to identify turmeric sources. In order to make it even simpler, we aimed to omit the use of sophisticated instruments like spectrophotometers, or Nuclear Magnetic Resonance spectrometers (NMR).<sup>9</sup> Instead, only common household tools including a document scanner, a digital camera, and a commercial black light were utilised to capture image data from chemical reactions performed on paper arrays. After some chemometric treatment, it was found that these simple tools were effective in identifying the sources of turmeric. Given its simple platform, this approach may also be a viable tool for simple geographical indications of other plants having a variety of chromophores.

## Experimental section

### Materials and chemicals

Fresh turmeric rhizomes (*Curcuma longa*) from four different sources, and turmeric powders from six different sources were obtained and used in this study. Fresh turmeric samples were purchased from local markets at each location. Sources outside Thailand were obtained *via* online purchase. The origins of these samples can be found in Table S1 in ESI.†

Chemical reagents and solvents were purchased from Sigma-Aldrich, Fluka, Carlo Erba, Chem-impex Ltd., May & Baker Ltd., Baker Analyzed, Merck and RCI Labscan (Thailand). Standard 98% curcumin was purchased from Chem-impex Ltd.

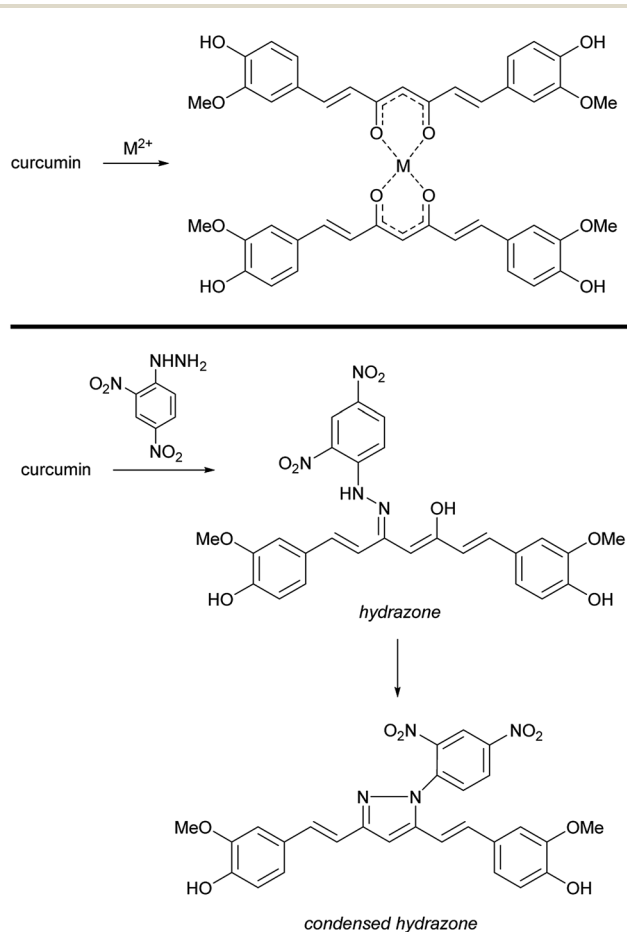
### Extraction procedure

One gram of oven-dried (72 hours at 50 °C), small cubic turmeric (or dry powder for powder samples) was added with methanol (5 mL), and the resulting mixture was heat at 65 °C for 4 h using AccuBlock™ digital dry bath heater (Labnet). Thereafter, methanol solution was removed, and the crude solid was added with dichloromethane (5 mL), followed by brief vortexing. The dichloromethane portion was then combined with the methanol portion, and the mixture was subject to rotary evaporation to remove all solvents. Dry crude was re-added with methanol to create a stock solution at 5 mg mL<sup>-1</sup>, with further dilutions depending on applications: HPLC-DAD = 1 mg mL<sup>-1</sup>, LC-MS = 0.25 mg mL<sup>-1</sup>, and reactions on paper arrays = 1 mg mL<sup>-1</sup>.

Standard 98% curcumin was diluted in methanol to create a stock solution at 1 mg mL<sup>-1</sup>, with further dilutions depending on applications: HPLC-DAD = 0.2 mg mL<sup>-1</sup>, LC-MS = 0.05 mg mL<sup>-1</sup>, and reactions on paper arrays = 0.2 mg mL<sup>-1</sup>.

### HPLC experiments

All HPLC experiments with a photodiode array detector (DAD) were performed with the following parameters. Model: Ultimate 3000, Thermo Fisher Scientific; column: VertiSep™ UPS C18 column, 4.6 × 50 mm, 3 μm; injection volume: 10 μL; mobile phases: solvent A = 0.1% aqueous formic acid, solvent B = 0.1%



**Scheme 1** Examples of chemical interactions and reactions of curcumin. Top: complexation with a metal ion. Bottom: hydrazone formation with 2,4-DNP.



formic acid in acetonitrile; flow rate: 0.5 mL min<sup>-1</sup>; time program: 30% B for 2 min, linear gradient to 90% B over 18 min, held at 90% B for 10 min, and a final decrease to 30% B.

**2,4-DNP reaction condition with curcumin samples.** 2,4-DNP stock solution (0.2 M) described below (under the section "Fabrication of paper arrays") was further diluted with methanol to 8 mM. Thereafter, 200  $\mu$ L of 5 mg mL<sup>-1</sup> turmeric sample was added with 300  $\mu$ L MeOH and 500  $\mu$ L of 8 mM 2,4-DNP solution. The final concentrations were 1 mg mL<sup>-1</sup> for crude turmeric, and 4 mM for 2,4-DNP. This solution was briefly vortexed and then incubated for 3 hours. The resulting solution was subject to HPLC analysis after filtration with 0.22  $\mu$ m nylon syringe filter.

### LC-MS experiments

All LC-MS experiments with a quadrupole time-of-flight (QTOF) detector were performed with the following parameters. UHPLC model: 1290 Infinity II, Agilent; mass spectrometer: SciEx X500R QTOF MS.; column: VertiSep™ UPS C18 column, 4.6  $\times$  50 mm, 3  $\mu$ m; injection volume: 10  $\mu$ L; mobile phases: solvent A = 0.1% aqueous formic acid, solvent B = 0.1% formic acid in acetonitrile; flow rate: 0.5 mL min<sup>-1</sup>; time program: the same as the HPLC-DAD experiments.

MS parameters: mass range = 80–800 *m/z*, positive mode; ion source gas 1 = 40 psi; ion source gas 2 = 50 psi; source temperature = 500  $^{\circ}$ C; spray voltage = 5500 V; declustering potential (DP) = 50 V; collision energy (CE) = 10 V. MS/MS parameters: mass range = 80–800 *m/z*, DP = 80 V; CE = 35  $\pm$  15 V. SciEx OS software was used to process all data.

**2,4-DNP reaction condition with curcumin samples.** The protocol was exactly the same as the one for HPLC-DAD analyses, but the final solution after 3 hour incubation was further diluted at 1 : 4 with methanol before analysis.

### Fabrication of paper arrays

A 20  $\times$  20 cm 1Chr Whatman chromatography paper was patterned as hydrophilic circular shapes (0.48 cm diameter) by wax printing with a Xerox ColorQube 8580 printer. The sheet was then cut into desired portions, and heated at 185  $^{\circ}$ C for 30 seconds. Thereafter, each sheet was attached with a transparent tape on the back side. This was followed by (1) dropping 5  $\mu$ L of a reagent into each well with 1 h incubation, and (2) dropping 5  $\mu$ L of a turmeric sample with 1 h incubation.

After the incubation step, a HP Deskjet Ink Advantage 2515 scanner (600 dpi) was used to obtain images under white light. This was then followed by obtaining images under 365 nm UV light using a Sony ILCE-5100 camera (settings: ISO 200, shutter speed at 1/4 s, and *F* value at 14) and a transilluminator (Vilber Lourmat 8W dual wavelength (312 & 365 nm)).

The detail about the preparation of each reagent array can be found in ESI†

### Chemometrics

The classification was performed using Linear Discrimination Analysis (LDA) with leave one out cross validation approach. The combinations of sensors were generated using full crossed

combinatorial function. All calculation software was in-house generated based on MATLAB version 9.4 (R2018a) platform (codes can be found in ESI†).

## Results and discussion

The experiment commenced with a simple step of curcumin extraction (details in the Experimental section). Briefly, 10 sources of turmeric (their origins can be found in Table S1†) were obtained – each was oven-dried at 50  $^{\circ}$ C for 72 hours. Thereafter, dried turmeric was added with methanol and heated at 65  $^{\circ}$ C for 4 hours. Methanol solution was then separated, and the crude turmeric was washed with dichloromethane. The two solutions were then combined, and the solvents were removed *in vacuo*. Finally, the crude was re-dissolved with methanol to create a 5 mg mL<sup>-1</sup> stock solution for further uses.

In order to better understand the nature of the extracts, the investigation started with some characterisations of the crudes before any chemical reaction. High-performance liquid chromatography (HPLC) experiments were conducted. As mentioned above, curcumins were known to absorb strongly at around 425 nm, and this could be easily seen in HPLC with 425 nm detection. Nevertheless, 250 nm was instead selected to reveal more peaks as curcumins can still be seen at this wavelength. In all cases, curcumin and demethoxy derivatives were clearly found (all chromatograms can be found in Table S2 in ESI†). For example, the Cur2 sample showed curcumin peaks at 12.8, 13.1, and 13.4 min, respectively (Fig. 2A). Also, the identities of these compounds were both verified from a comparison

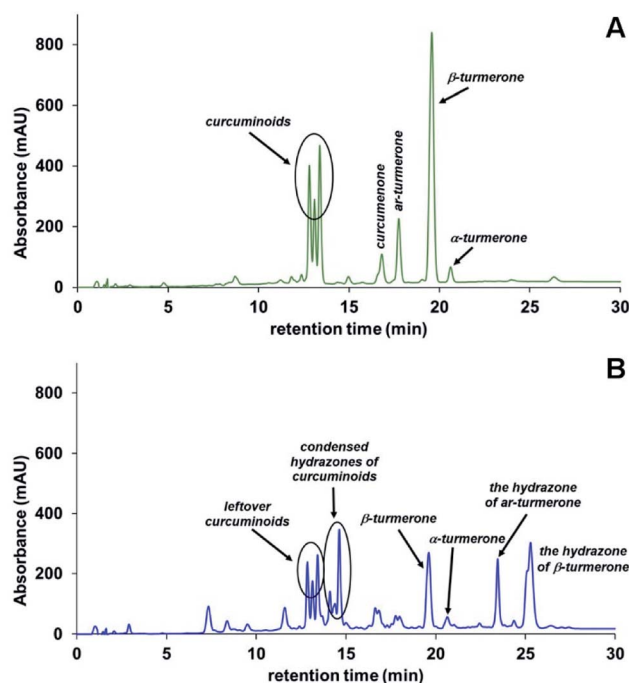


Fig. 2 HPLC chromatograms of (A) a crude extract of the Cur2 sample; (B) the same crude extract after subjecting to a reaction with 2,4-DNP for 3 hours. The detection wavelength was 250 nm. Some prominent compounds were also outlined.



with an authentic standard, and from liquid chromatography – tandem mass spectrometry (LC-MS) experiments (Table S3†), which accurately revealed the highly accurate  $m/z$  values of all curcumin derivatives at these same positions. Interestingly, some other components absorbing at 250 nm were also visible in this exemplary extract, *e.g.*, at 16.8, 17.8 and 19.6 min (Fig. 2A). MS data (molecular masses and certain MS/MS fragmentation patterns), along with comparisons with previous studies,<sup>39–41</sup> suggested that most of these compounds are known sesquiterpenes typically found in turmeric such as turmerone species (Table S3†). Other minor components such as dihydrocurcumin (reduced curcumin derivatives) could also be detected by MS although these are usually not clearly visible in HPLC with UV-vis detection.

Importantly, both the amounts of total curcumins and non-curcumin components obviously differ from one source to another (Table S2†). In fact, these differences were confirmed to be sufficient for differentiating sources of turmeric in a previous study using HPLC.<sup>9</sup> In our case, we hypothesized that these differences in chemical contents also affect the reactivity of curcumins in reacting with various reagents, which in turn may be used as another means of differentiation. To test this hypothesis, we proceeded to perform imine formation reaction (Experimental section) with 2,4-DNP. As shown in Fig. 2B, several new peaks appeared. Although identifying all newly formed species is not relevant to our main goal, some peaks were characterised by accurate MS (Table S3†). For instance, apart from the remaining 2,4-DNP and curcumin derivatives, hydrazone derivatives of several previously detected curcumins could be seen, *e.g.*, peaks at 16.6 and 18.0 min (entries 11–16 in Table S4†). Apart from these hydrazones, further condensation and tautomerization also resulted in putative cyclic products (denoted “condensed hydrazone” in Scheme 1) – this could be unambiguously confirmed by MS at 14.1, 14.4, and 14.6 min for Cur2 sample. As a comparison, a similar reaction was conducted with the Cur3 sample, which clearly showed different peak patterns (Table S2 in ESI†). This finding implies that our hypothesis is likely correct, and an array of sufficient numbers of chemical reactions may allow indications of turmeric sources.

Encouraged by the aforementioned results, chemical arrays were then fabricated. This was performed by wax-printing a simple circular pattern on laboratory papers. Each circular area was then used to drop a variety of chemical reagents, which were selected based on known evidences of aforementioned spectroscopic changes<sup>26–30,34–38</sup> and in-house confirmation experiments (see below). Lastly, a turmeric extract solution to be investigated was dropped on each reaction well for testing, followed by 1 hour incubation at ambient environment. As shown in Fig. 3A, some interactions and reactions clearly changed the colour profile of the original turmeric solutions. Prominent examples include the red colour from basic condition (pH 12),<sup>42</sup> the bright red rosocyanine produced from a well-known complexation with  $\text{H}_3\text{BO}_3$  (produced from  $\text{B}_4\text{O}_7^{2-}$  and  $\text{H}_2\text{SO}_4$ ),<sup>26,27</sup> and orange-brown colour generated from the complexes between curcumin with  $\text{Fe}^{2+}$ .<sup>28</sup> Furthermore, the observation of fluorescence also revealed extra information as

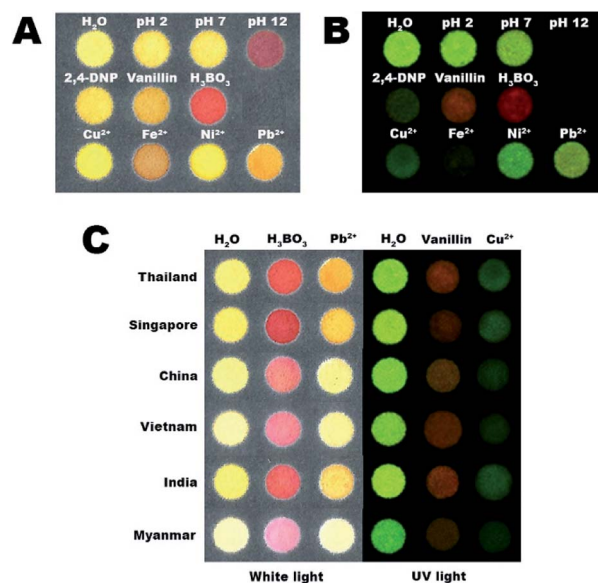


Fig. 3 Paper arrays of chemical reactions probed under (A) white light, (B) 365 nm UV light. Details of specific concentrations and other conditions of each reagent can be found in ESI.† The panel in (C) showed side-by-side comparison of reactions with  $\text{H}_3\text{BO}_3$ ,  $\text{Pb}^{2+}$  (white light – left half), vanillin, and  $\text{Cu}^{2+}$  (UV light – right half) from turmeric sources from various countries.

some reagents could reduce the fluorescence intensity from curcumins including  $\text{Cu}^{2+}$ ,<sup>43</sup>  $\text{Fe}^{2+}$ , and 2,4-DNP (Fig. 3B). Vanillin and  $\text{H}_3\text{BO}_3$  resulted in both reduction of emission and a shift of emission wavelength. To further confirm the potential of these reagents, further analyses were also conducted. First, a representative set of reaction arrays (based on 98% curcumin) was prepared, and the reaction profiles of the responses of this curcumin sample to selected reagents in digital images were converted into numerical data by ImageJ processing software. This was then plotted as bar graphs as shown in Fig. S1.† It is evident from these data that each reagent gave different responses, both as the total intensity values, and in each colour channel. Furthermore, despite being not directly critical to our applications, the limits of detection (LOD) of some reagents to the standard curcumin were also determined to give some general ideas of how sensitively each reagent responds to curcumins. As shown in Fig. S2–S6,† various reagents gave various LOD around mid to high micromolar ranges, with a general trend being that the fluorescence responses unsurprisingly provided better sensitivities than did white-light responses. Anyway, it should be emphasised herein that the sensitivities may not be utmost important as this can be overcome by adding more turmeric samples into each reaction well. Instead, the fact that each reagent reacted differently (thus giving different LOD and slope profiles) was perhaps more essential. Combined together, these data showed some promise for differentiation of turmeric sources, as mere side-by-side comparison (Fig. 3C) already exerted different reactivity patterns from different turmeric sources.

To allow for practical differentiations, all data were subject to chemometric treatments. This could be done by first



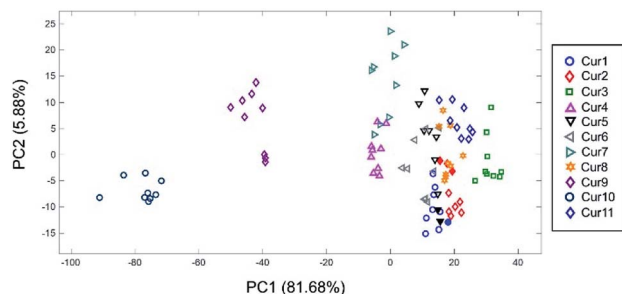


Fig. 4 A two-dimensional PC score plot for the combination of 8 reagents ( $\text{H}_2\text{O} + \text{pH } 2 + 2,4\text{-DNP} + \text{vanillin} + \text{H}_3\text{BO}_3 + \text{Fe}^{2+} + \text{Ni}^{2+} + \text{Pb}^{2+}$ ) in discriminating 11 turmeric sources. Filled items represented indistinguishable samples.

converting reaction profiles from digital photos into numerical data by ImageJ processing software. The resulting data in the form of red, green, and blue (RGB) numerical values on both visualisation modes (white and UV lights) of each reagent spot were then used to create a multidimensional data set. This consisted of 99 samples (11 turmeric sources with 9 replicates) and 66 variables (3 RGB numerical data, 2 visualization modes and 11 reagent wells), which were then used to investigate the best combination from all possible combinations of reagent arrays (2047 combinations – raw data are provided in ESI†). Notably, the discovery of this best combination of reagents was made possible by the use of chemometrics, which permitted relatively rapid analysis on the prediction accuracies of all reagent combinations (Fig. S7†). This resulted in a set of 8 reagents ( $\text{H}_2\text{O} + \text{pH } 2 + 2,4\text{-DNP} + \text{vanillin} + \text{H}_3\text{BO}_3 + \text{Fe}^{2+} + \text{Ni}^{2+} + \text{Pb}^{2+}$ ) that provided a satisfactorily maximum 94% prediction accuracy. To visualize the relation of samples, principal component analysis (PCA) was performed on the data using only the aforementioned 8 selected reagents. A representative two-dimensional PC plot (Fig. 4) provided clear differentiations on certain samples, with the most prominent ones being Cur9 and Cur10. The only problematic case was between Cur5 and Cur6, both of which were from the same country (Thailand). No other obscure result was obtained for samples from different countries.

In essence, chemometric treatment aided in demonstrating the power of reagent arrays, where it unambiguously showed that combinations of reagents, but not just any individual reagent, were needed for better predictions on the geographical profiles of turmeric samples. On the contrary, chemometrics helped in reducing the time and effort of conducting experiments by clearly suggesting the optimum set of experiments, which are not necessarily the ones with highest numbers of variables. This could be clearly illustrated in a heat-map chart in Fig. 5. Matched colours on each row to the reference panel on the right panel indicated that those reagents (or combinations thereof) could correctly indicate the origin of the sample. Clearly, the suggested eight-reagent combination obtained from chemometric treatment gave the highest number of matched colours, which was significantly higher than any individual reagent or even 11 reagents.

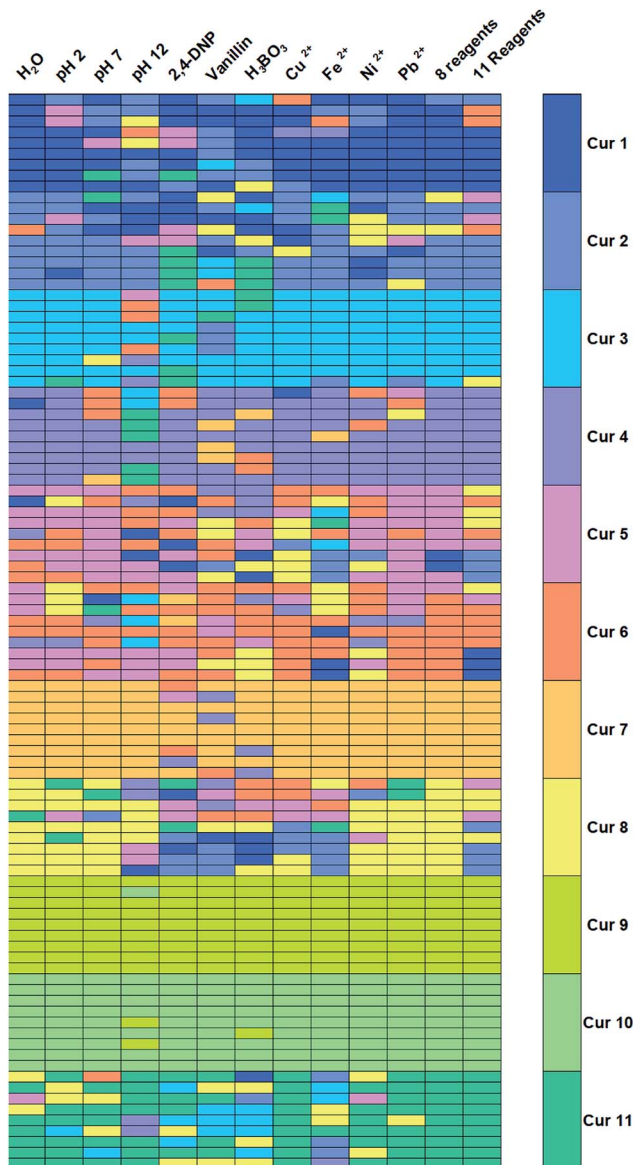


Fig. 5 A heat-map chart as a representation of correctness in predicting the origins of turmeric samples. Matched colours from the left panel to the reference panel on the right indicated that the respective reagents could correctly predict the origin of the sample (8 reagents were  $\text{H}_2\text{O} + \text{pH } 2 + 2,4\text{-DNP} + \text{vanillin} + \text{H}_3\text{BO}_3 + \text{Fe}^{2+} + \text{Ni}^{2+} + \text{Pb}^{2+}$  – this particular combination was found from extensive evaluations of prediction accuracies *via* chemometric treatments).

## Conclusions

In conclusion, we demonstrated herein the synergistic utilization of chemical arrays and chemometric approach in indicating the geographical origins of turmeric samples. Without the need for sophisticated instruments, our method provided up to 94% accuracy of geographical prediction. Furthermore, this method is also theoretically applicable to other foods and plants having chromophores, thus underscoring the impact of this method to broader usages.



## Conflicts of interest

There are no conflicts to declare.

## Acknowledgements

This work was supported by the Thailand Research Fund (MRG5980037). MR and TS thank the Development and Promotion of Science and Technology Talented Project (DPST) for their Ph. D. Scholarships.

## Notes and references

- B. Dogan and U. Gokovali, *Procedia Soc. Behav. Sci.*, 2012, **62**, 761–765.
- M. d. L. Medeiros, C. S. Passador and J. L. Passador, *RAI Revista de Administração e Inovação*, 2016, **13**, 315–329.
- D. M. A. M. Luykx and S. M. van Ruth, *Food Chem.*, 2008, **107**, 897–911.
- V. Uričková and J. Sádecká, *Spectrochim. Acta, Part A*, 2015, **148**, 131–137.
- F. J. Monahan, O. Schmidt and A. P. Moloney, *Meat Sci.*, 2018, **144**, 2–14.
- S. Yudthavorasit, K. Wongravee and N. Leepipatpiboon, *Food Chem.*, 2014, **158**, 101–111.
- A. G. Potorti, G. Di Bella, A. F. Mottese, G. D. Bua, M. R. Fede, G. Sabatino, A. Salvo, R. Somma, G. Dugo and V. Lo Turco, *J. Food Compos. Anal.*, 2018, **69**, 122–128.
- E. Durán-Guerrero, F. Chinnici, N. Natali and C. Riponi, *J. Sci. Food Agric.*, 2015, **95**, 2395–2403.
- H. A. Gad and A. Bouzabata, *Food Chem.*, 2017, **237**, 857–864.
- S. Zhang, Y. Wei, S. Wei, H. Liu and B. Guo, *Int. J. Food Sci. Technol.*, 2017, **52**, 457–463.
- R. Urvieta, F. Buscema, R. Bottini, B. Coste and A. Fontana, *Food Chem.*, 2018, **265**, 120–127.
- N. Ali and A.-E. Soheil, *Curr. Pharm. Des.*, 2013, **19**, 2032–2046.
- S. Prasad, S. C. Gupta, A. K. Tyagi and B. B. Aggarwal, *Biotechnol. Adv.*, 2014, **32**, 1053–1064.
- K. Priyadarsini, *Molecules*, 2014, **19**, 20091.
- S. Ghosh, S. Banerjee and P. C. Sil, *Food Chem. Toxicol.*, 2015, **83**, 111–124.
- D. Mathew and W.-L. Hsu, *J. Funct. Foods*, 2018, **40**, 692–699.
- S. Sundar Dhillip Kumar, N. Houreld and H. Abrahamse, *Molecules*, 2018, **23**, 835.
- E. Burgos-Morón, J. M. Calderón-Montaño, J. Salvador, A. Robles and M. López-Lázaro, *Int. J. Cancer*, 2010, **126**, 1771–1775.
- K. M. Nelson, J. L. Dahlin, J. Bisson, J. Graham, G. F. Pauli and M. A. Walters, *J. Med. Chem.*, 2017, **60**, 1620–1637.
- A. Mukerjee, T. J. Sørensen, A. P. Ranjan, S. Raut, I. Gryczynski, J. K. Vishwanatha and Z. Gryczynski, *J. Phys. Chem. B*, 2010, **114**, 12679–12684.
- D. Patra and C. Barakat, *Spectrochim. Acta, Part A*, 2011, **79**, 1034–1041.
- C. Boga, C. Delpivo, B. Ballarin, M. Morigi, S. Galli, G. Micheletti and S. Tozzi, *Dyes Pigm.*, 2013, **97**, 9–18.
- H.-J. Kim, D.-J. Kim, S. N. Karthick, K. V. Hemalatha, C. J. Raj, S. ok and Y. choe, *Int. J. Electrochem. Sci.*, 2013, **8**, 8320–8328.
- Y. Zhou and R.-C. Tang, *Dyes Pigm.*, 2016, **134**, 203–211.
- S. Wanninger, V. Lorenz, A. Subhan and F. T. Edelmann, *Chem. Soc. Rev.*, 2015, **44**, 4986–5002.
- E. W. Grotheer, *Anal. Chem.*, 1979, **51**, 2402–2403.
- E. Carrilho, S. T. Phillips, S. J. Vella, A. W. Martinez and G. M. Whitesides, *Anal. Chem.*, 2009, **81**, 5990–5998.
- M. P. Bhat, M. P. Patil, S. K. Nataraj, T. Altalhi, H.-Y. Jung, D. Losic and M. D. Kurkuri, *Chem. Eng. J.*, 2016, **303**, 14–21.
- S. Raj and D. R. Shankaran, *Sens. Actuators, B*, 2016, **226**, 318–325.
- G. Xu, J. Wang, G. Si, M. Wang, X. Xue, B. Wu and S. Zhou, *Sens. Actuators, B*, 2016, **230**, 684–689.
- L. R. Uppström, *Anal. Chim. Acta*, 1968, **43**, 475–486.
- M. S. Refat, *Spectrochim. Acta, Part A*, 2013, **105**, 326–337.
- F.-S. Yan, J.-L. Sun, W.-H. Xie, L. Shen and H.-F. Ji, *Nutrients*, 2018, **10**, 28.
- L. A. Jones, C. K. Hancock and R. B. Seligman, *J. Org. Chem.*, 1961, **26**, 228–232.
- S. Uchiyama, Y. Inaba and N. Kunugita, *J. Chromatogr. B: Biomed. Sci. Appl.*, 2011, **879**, 1282–1289.
- S. M. van Leeuwen, L. Hendriksen and U. Karst, *J. Chromatogr. A*, 2004, **1058**, 107–112.
- S. K. Sarkar and R. E. Howarth, *J. Agric. Food Chem.*, 1976, **24**, 317–320.
- J. S. Zhang, J. Guan, F. Q. Yang, H. G. Liu, X. J. Cheng and S. P. Li, *J. Pharm. Biomed. Anal.*, 2008, **48**, 1024–1028.
- X.-G. He, L.-Z. Lin, L.-Z. Lian and M. Lindenmaier, *J. Chromatogr. A*, 1998, **818**, 127–132.
- F. Liu, X. Bai, F.-Q. Yang, X.-J. Zhang, Y. Hu, P. Li and J.-B. Wan, *Chin. Med.*, 2016, **11**, 21.
- I.-C. Chao, C.-M. Wang, S.-P. Li, L.-G. Lin, W.-C. Ye and Q.-W. Zhang, *Molecules*, 2018, **23**, 1568.
- N. Pourreza and H. Golmohammadi, *Talanta*, 2015, **131**, 136–141.
- M. H. M. Leung, D.-T. Pham, S. F. Lincoln and T. W. Kee, *Phys. Chem. Chem. Phys.*, 2012, **14**, 13580–13587.

